Temperature dependence of acoustic harmonics generated by nonlinear ultrasound wave propagation in water at various frequencies

Borna Maraghechi
Department of Physics, Ryerson University, 350 Victoria Street, Toronto, Ontario M5B 2K3, Canada

Mojtaba H. Hasani
Department of Biomedical Engineering, Amirkabir University of Technology, 424 Hafez Avenue, Tehran, Iran

Michael C. Kolios[a] and Jahan Tavakkoli[a),b)]
Department of Physics, Ryerson University, 350 Victoria Street, Toronto, Ontario M5B 2K3, Canada

(Received 28 May 2015; revised 13 January 2016; accepted 1 April 2016; published online 6 May 2016)

Ultrasound-based thermometry requires a temperature-sensitive acoustic parameter that can be used to estimate the temperature by tracking changes in that parameter during heating. The objective of this study is to investigate the temperature dependence of acoustic harmonics generated by nonlinear ultrasound wave propagation in water at various pulse transmit frequencies from 1 to 20 MHz. Simulations were conducted using an expanded form of the Khokhlov–Zabolotskaya–Kuznetsov nonlinear acoustic wave propagation model in which temperature dependence of the medium parameters was included. Measurements were performed using single-element transducers at two different transmit frequencies of 3.3 and 13 MHz which are within the range of frequencies simulated. The acoustic pressure signals were measured by a calibrated needle hydrophone along the axes of the transducers. The water temperature was uniformly increased from 26 °C to 46 °C in increments of 5 °C. The results show that the temperature dependence of the harmonic generation is different at various frequencies which is due to the interplay between the mechanisms of absorption, nonlinearity, and focusing gain. At the transmit frequencies of 1 and 3.3 MHz, the harmonic amplitudes decrease with increasing the temperature, while the opposite temperature dependence is observed at 13 and 20 MHz. [http://dx.doi.org/10.1121/1.4946898]

[OAS] Pages: 2475–2481

I. INTRODUCTION

Noninvasive thermometry is needed to monitor the temperature change in the heated region during thermal treatments in order to improve the treatment efficacy and safety. Ultrasound is an attractive option for temperature mapping since it is non-ionizing, portable, and is inexpensive. Several ultrasonic techniques have been proposed for noninvasive tissue thermometry.[1,2] In order to noninvasively estimate the temperature using ultrasound, a temperature sensitive acoustic parameter is required. The temperature could be estimated by knowing the temperature dependence of the parameter and tracking changes in that parameter during heating.

Acoustic pulses with relatively high-pressure progressively get distorted as they propagate and generate higher harmonics. This effect increases with increasing frequency, source pressure, and focusing gain of the beam at a given propagation distance.[3] Finite-amplitude effects of nonlinear propagation of ultrasound waves are used in various diagnostic and therapeutic applications of ultrasound.[4,5]

Tissue Harmonic Imaging is an imaging technique in which a pulse with a center frequency of f_0 is transmitted and the signal containing the second harmonic ($2 \times f_0$) is received to form an image.[4,5] Superharmonic imaging uses the combination of the third, fourth, and fifth harmonics of the received signal to image.[6] It has been shown that imaging with these harmonics improves the spatial resolution and reduces the aberration and reverberation artifacts of the image.[4–6]

Acoustic nonlinearity parameter imaging has been applied for tissue characterization. The value of the acoustic nonlinearity parameter (B/A) of fatty tissues is typically twice that of non-fatty tissues.[7] Zhang *et al.*[7] showed that B/A can provide information about the composition of the tissue. They generated B/A images of biological specimens such as porcine normal and fatty liver tissues, and porcine fat tissue.

Studies have shown that B/A is temperature dependent and it could be considered as a basis for an ultrasound-based method for noninvasive temperature estimation.[8,9] The B/A is about 4 times more temperature sensitive compared to the speed of sound and thermal expansion in water.[8] van Dongen and Verweij simulated the nonlinear propagation of acoustic waves in glycerol using the lossless form of the Burgers equation.[8] They showed that the harmonic pressure amplitudes are temperature dependent and could potentially be considered as suitable parameters for noninvasive ultrasound thermometry. However, the lossless form of Burgers

[a)]Also at: Institute for Biomedical Engineering, Science and Technology (iBEST), Keenan Research Centre for Biomedical Science, St. Michael's Hospital, Toronto, Ontario, M5B 1W8, Canada.
[b)]Electronic mail: jtavakkoli@ryerson.ca

equation is the simplest model that describes only the effect of nonlinearity for acoustic plane waves of finite amplitude. Both[10] simulated an acoustic plane wave propagating in water in order to study the temperature dependence of harmonics. The simulations were performed using two different solutions of Burgers equation known as Keck-Beyer and Fubini for lossy and lossless media, respectively.[3,10] A monochromatic 1 MHz source with a pressure of 1 MPa was used in the study. The author showed that the harmonics are weakly sensitive to temperature and a minimum in the harmonic pressure value occurs at around 45 °C. It is worth noting that neither of the simulation studies mentioned did take into account the combined effects of diffraction, absorption, and nonlinearity—all of which change the harmonics amplitude of the propagating waves.

We have recently shown that the pressure amplitude and the energy content of the backscattered fundamental frequency, the second and the third harmonics generated by nonlinear ultrasound propagation in tissue-mimicking gel phantoms, and *ex vivo* bovine muscle tissues are highly sensitive to temperature, when the acoustic harmonics were generated by transmitting a 13-MHz pulse using a high-frequency ultrasound imaging scanner.[11] It was also demonstrated that higher harmonics have a higher sensitivity to temperature.

The Khokhlov–Zabolotskaya–Kuznetsov (KZK) nonlinear wave equation is a well-established model for finite-amplitude wave propagation.[3,12–14] The KZK equation is a parabolic approximation of the Westervelt nonlinear wave equation that consists of terms to account for diffraction, absorption, and nonlinearity.[3] The diffraction term accounts for the finite dimensions of the source and the attenuation term considers the heat conduction and viscosity of the medium. The nonlinear term accounts for the nonlinear propagation of the finite-amplitude wave.

In this study, the temperature dependence of harmonic amplitudes generated by nonlinear ultrasound wave propagation in water is examined at various pulse transmit frequencies from 1 to 20 MHz using the KZK wave equation. Nonlinear ultrasound wave propagation simulations were performed using a time-domain numerical solution of a modified KZK nonlinear wave equation that accounts for temperature dependent medium parameters. The simulation results are compared with measurements. Measurements were performed using two single element transducers at frequencies of 3.3 and 13 MHz.

The main objective of this study is to investigate and understand the mechanisms of action of harmonics generation as a function of temperature at various frequencies in water which is a simple, homogeneous, and more controlled medium compared to tissue. Soft tissues exhibit additional complexities such as significant structural heterogeneity that change as a function of time (tissue decay) and temperature. Moreover, water was chosen in experiments and simulations because the values for acoustic parameters (attenuation coefficient, speed of sound, density, and B/A) of water were available as a function of temperature in the literature. Currently, there are limited amount of information on the temperature dependence of these acoustic parameters for soft tissue which we need as inputs to our simulation model.[9,15,16]

II. MATERIALS AND METHODS

A. Temperature dependent nonlinear ultrasound wave propagation model

Nonlinear ultrasound wave propagation simulations were performed using a time-domain numerical solution of a modified KZK nonlinear wave equation in which temperature dependence of the medium parameters was included. The dimensionless form of the temperature-dependent KZK equation for focused sources could be given as[13]

$$\frac{\partial P}{\partial \sigma} = \frac{1}{4G(T)}\int_{-\infty}^{\tau}\left(\frac{b}{a}\frac{\partial^2 P}{\partial X^2}+\frac{a}{b}\frac{\partial^2 P}{\partial Y^2}\right)d\tau' + A(T)\frac{\partial^2 P}{\partial \tau^2} + N(T)\left(P\frac{\partial P}{\partial \tau}\right), \quad (1)$$

where P is the transformed source pressure amplitude defined as $P=(p/p_0)$ which p is the sound pressure in the Cartesian coordinates and p_0 is the source pressure amplitude. $\sigma = z/d$ is the dimensionless z axis (axial distance divided by the focal length d) for a source with characteristic sizes of a and b in the x and y directions with an angular frequency of ω_0. X and Y are the transformed transverse coordinates ($X=x/a$, $Y=y/b$) and T is the temperature. $G(T)$ is the focusing gain defined as

$$G(T) = \frac{z_0(T)}{d} = \frac{\pi f_0 ab}{c_0(T)d}, \quad (2)$$

where z_0 is the Rayleigh distance. $A(T)$ is the absorption parameter defined as

$$A(T) = \alpha(T)d = \alpha_0(T)f_0^2 d, \quad (3)$$

where α_0 is the pressure absorption coefficient. $N(T)$ is the nonlinear parameter defined as

$$N(T) = \frac{d}{\bar{z}(T)} = \frac{\beta(T)2\pi f_0 p_0}{\rho_0(T)c_0^3(T)}d, \quad (4)$$

where $\bar{z}$ is the plane wave shock formation distance. c_0 and ρ_0 are the small signal speed of sound and the medium density, respectively. τ is the transformed retarded time defined as $\tau=\omega_0 t'$ where t' is the retarded time ($t'=t-z/c_0$). The terms on the right-hand side of Eq. (1) account for diffraction, nonlinearity, and thermoviscous absorption, respectively.[13]

The source boundary condition was defined as $p=p_0 f(t+x^2/2c_0d_x+y^2/2c_0d_y)\ g(x,\ y)\ \xi(x,y)$, $z=0$, where $f(t)$, $g(x,\ y)$, and $\xi(x,\ y)$ are the source temporal excitation, the source spatial aperture function, and the source apodization function, respectively. By using the variable transformations and dimensionless variables, the source boundary condition could be rewritten as $P=f(\tau+G_xX^2+G_yY^2)\ g(X,\ Y)\ \xi(X,\ Y)$, $\sigma=0$, where $G_x=G\ bd/ad_x$ and $G_y=G\ ad/bd_y$ are the directional focusing gains in the x and y directions, respectively.

For a circular source, the function $g(X, Y)$ can be written as

$$g(X,Y) = \begin{cases} 1 & X^2 + Y^2 \le 1, \\ 0 & \text{otherwise.} \end{cases} \quad (5)$$

In the selection of boundary values, the extent of spatial domains, X_{max} and Y_{max}, were chosen large enough to minimize reflections due to artificial boundary conditions. The time window was also large enough to encompass the entire waveform, including delayed edge waves.[13]

Nonlinear propagation of 9 and 7 cycle pulses at 3.3 and 13 MHz in water with source pressure amplitudes of 0.26 and 0.05 MPa, respectively, and for the same transducer geometries used in our experiments were simulated. The source pressure amplitudes used in simulations were selected in order to achieve similar pressure and a similar degree of nonlinear waveform distortion as to that obtained in the experiments at the transducer focus and along the acoustic axes when water was at the baseline temperature of 26 °C. Simulations for the 1 and 20 MHz pulses were performed using the same parameters as those at 3.3 and 13 MHz, respectively. The source pressure waveform was a Gaussian envelope pulse given as

$$P = \exp\left[-\left(\frac{\tau}{n\pi}\right)^2\right] \sin\tau, \quad (6)$$

where n is the number of cycles. In order to replicate the effects induced by raising the temperature of water from 26 °C to 46 °C, the empirical temperature dependent values of four acoustic medium parameters at each temperature were used as an input to the simulation. The values of sound speed, medium's density, absorption coefficient, and the B/A as a function of temperature in water were obtained from published data[8,14,17] and are shown in Fig. 1.

In order to take into account the spatial averaging effect of the hydrophone, harmonics were averaged over a circular area corresponding to virtual area of the hydrophone used in the experiments.[18,19] The change in the peak pressure amplitudes of the harmonics and their ratios were analyzed at each simulated water temperature from 26 °C to 46 °C in increments of 5 °C.

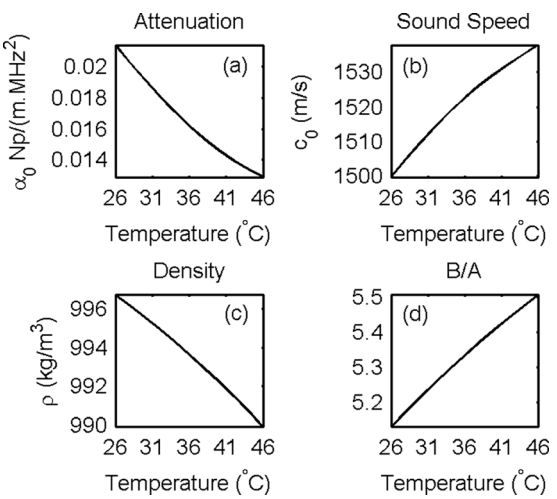

FIG. 1. The (a) attenuation coefficient (Ref. 14), (b) speed of sound (Ref. 14), (c) density (Ref. 8), and (d) B/A (Ref. 17) as empirical functions of temperature in water.

B. Experiments

A broadband single-element transducer with center frequency of 5 MHz (Matec, Northborough, MA) was used to generate pulses at 3.3 MHz. The transducer had a diameter of 6 mm and a focal length of 3 cm. The transducer was driven by an arbitrary function generator (Model AFG3101; Tektronix, Beaverton, OR) through a class-A broadband radio frequency power amplifier (Model 325LA; E&I, Rochester, NY), with a frequency range of 250 kHz to 150 MHz and a nominal gain of 50 dB. A high-frequency ultrasound imaging scanner (Vevo® 770, Visualsonics Inc., Toronto, ON, Canada) with a 25 MHz center frequency wide-band single-element transducer (RMV-710B, 7.1 mm diameter, 15 mm focal length) was used to generate pulses at 13 MHz. Acoustic harmonics were generated by transmitting pulse trains of 15-cycle length at 3.3 and 13 MHz with focal positive peak pressures of approximately 0.6 and 0.9 MPa, respectively, in water at 26 °C. The purpose of choosing these pressures was to have reasonable signal-to-noise ratio values for the first, second, and third harmonics.

The acoustic pressure signals were measured along the axes of the transducers by a calibrated needle hydrophone with an active element diameter of 400 μm (Model HNA-0400; ONDA Corporation, Sunnyvale, CA). Water was placed in a 2.5 cm diameter cylindrical container with a transparent window at the bottom. Water temperature was uniformly elevated from 26 °C to 46 °C in increments of 5 °C by the flow of hot water around the container. Hot water was pumped from a controlled circulating water bath (Haake DC10, Thermo Electron Corp., Newington, NH) using a peristaltic pump (Masterflex® L/S®, Cole Parmer, Chicago, IL). The 5 MHz transducer was immersed in a water tank for coupling with the container. The RMV-710B transducer was coupled with the container using acoustic gel. A schematic of the experimental setup is shown in Fig. 2. The received signal detected by the hydrophone was recorded with a 350 MHz digital oscilloscope (Model 7032A;

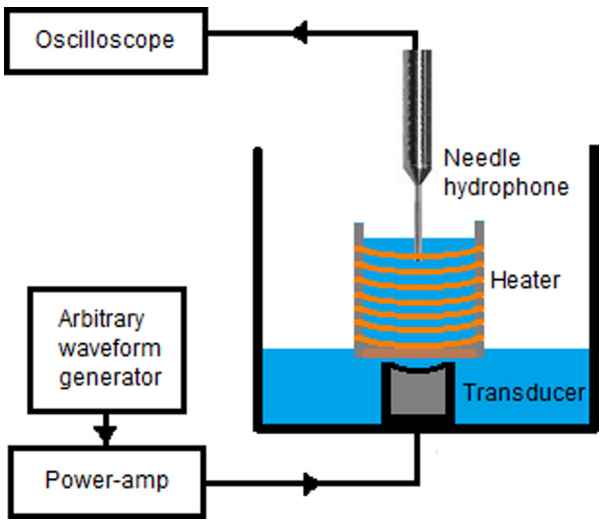

FIG. 2. (Color online) Schematic of the experimental setup at 3.3 MHz.

Agilent Technologies, Santa Clara, CA) and analyzed offline. The pressure amplitudes of the fundamental frequency (p_1), and its harmonics [second (p_2), third (p_3)] generated by nonlinear ultrasound propagation were obtained by calculating the frequency spectrum of the measured acoustic pressure signals. The peak pressure harmonic amplitudes and their ratios (p_2/p_1 and p_3/p_1) were analyzed as a function of water temperature and transducers transmit frequencies. The experiments were repeated 12 times at each transmit frequency and temperature.

III. RESULTS

The simulated and measured waveforms and their frequency spectra at both transmit frequencies of 3.3 and 13 MHz are shown in Figs. 3 and 4, respectively. The measured and simulated pressure amplitudes of the lowest three harmonic components along the axis of the ultrasound beam with transmit frequencies of 3.3 and 13 MHz are shown in Fig. 5. The average and standard deviation of the harmonic amplitudes and their ratios were calculated for each temperature. Figures 6 and 7 show the simulated and measured percentage changes in the pressure harmonic amplitudes (p_1, p_2, and p_3) and their ratios (p_2/p_1 and p_3/p_1) with temperature, respectively, at various frequencies.

IV. DISCUSSION

The results obtained from measurements and simulations shown in Figs. 6 and 7 demonstrate that the harmonic pressure amplitudes and their ratios decrease with temperature for the pulse transmit frequency of 1 and 3.3 MHz. On the other hand, at 13 and 20 MHz transmit frequencies, the harmonics and their ratios show an increasing trend as the temperature increases from 26 °C to 46 °C.

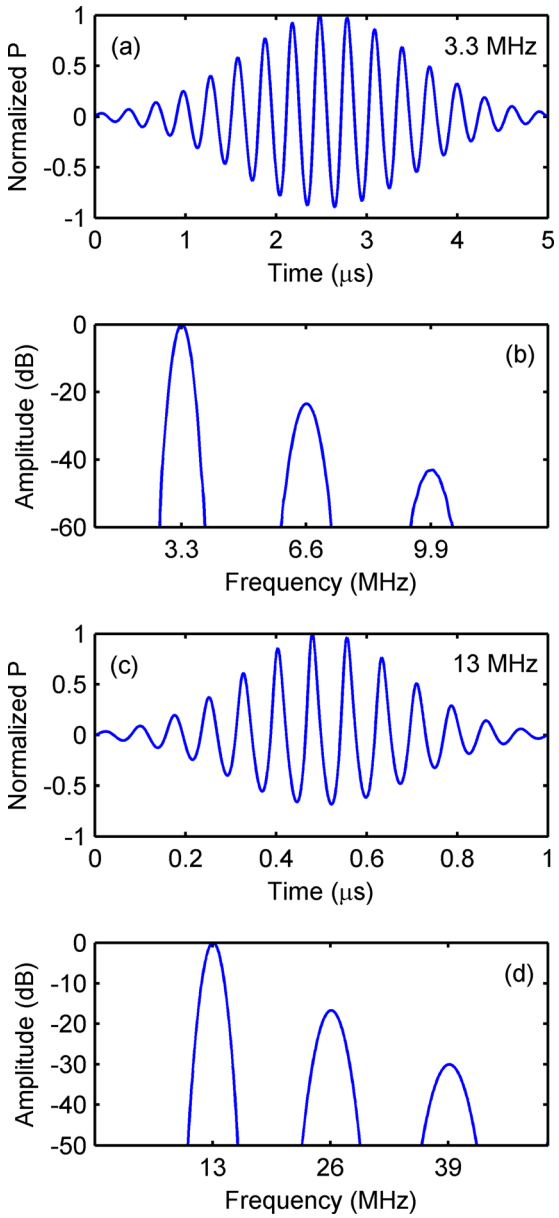

FIG. 3. (Color online) Simulated normalized focal pressures and the magnitude of their spectra for pulses with transmit frequencies of (a) and (b) 3.3 MHz and (c) and (d) at 13 MHz, respectively, at the initial temperature (26 °C).

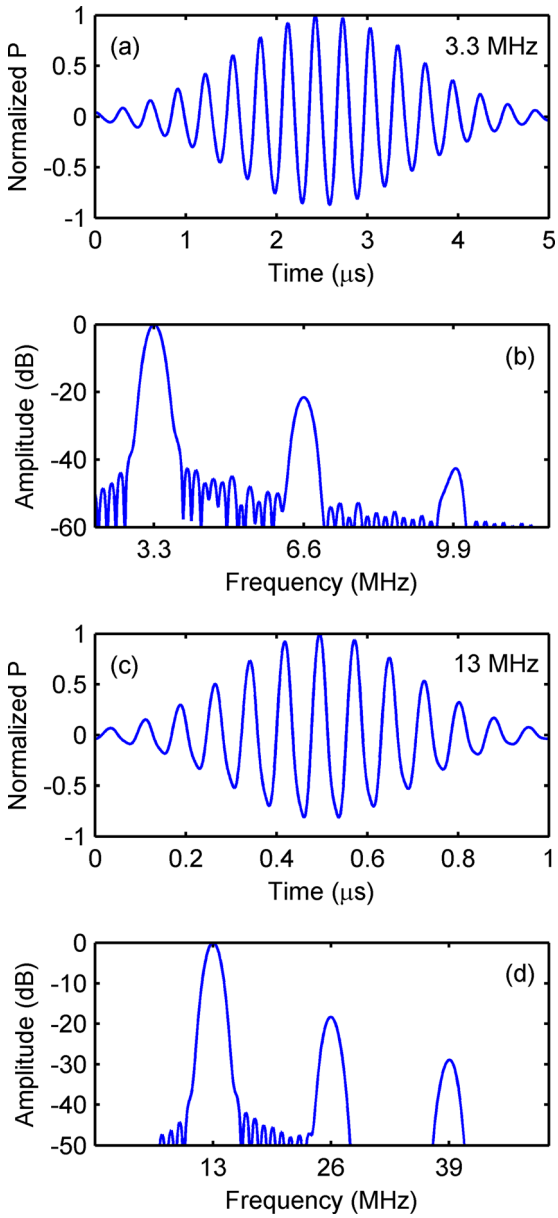

FIG. 4. (Color online) Measured normalized focal pressures and the magnitude of their spectra for pulses with transmit frequencies of (a) and (b) 3.3 MHz and (c) and (d) 13 MHz, respectively, at the initial temperature (26 °C).

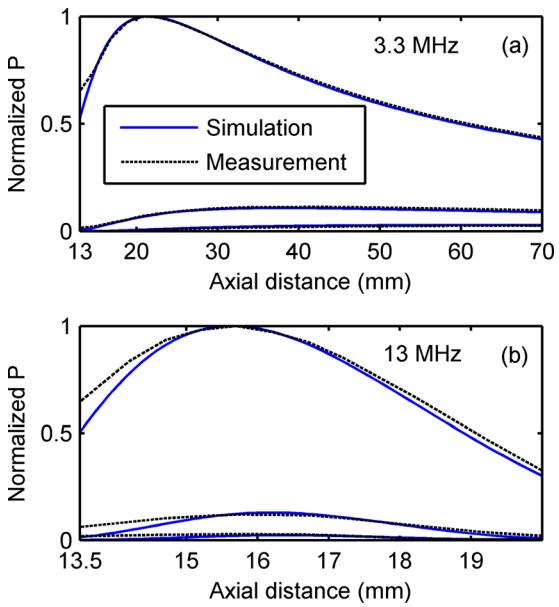

FIG. 5. (Color online) Measured (dotted line) and simulated (solid line) normalized pressure amplitudes of the lowest three harmonic components along the axis of the beam with transmit frequencies of (a) 3.3 MHz and (b) 13 MHz at the initial temperature (26 °C).

The results can be explained by the interplay between the temperature dependence of the absorption, nonlinearity, and focusing gain. The relative importance of nonlinearity and absorption in the KZK model used in this study is determined by the dimensionless parameters of nonlinearity (N) and absorption (A), respectively. The ratio $\Gamma = N/A$ is defined as the Gol'dberg number, which provides a measure of balance between the nonlinear and the absorption processes.[12] Duck[4] stated that when $\Gamma \gg 1$ the nonlinear process dominates and when Γ is close to 1.0, the effects of nonlinearity and absorption are comparable. The focusing gain (G) is the peak value of p/p_0 at the geometric focus in the absence of absorption and nonlinearity.[12]

Figure 8 shows the percentage changes in A, N, Γ, and G as a function of temperature for pulse transmit frequencies of 1, 3.3, 13, and 20 MHz.

As the temperature increases from 26 °C to 46 °C, the absorption parameter decreases by about 40% whereas the nonlinear parameter and the focusing gain decrease by about −1.6% and −2.5%, respectively (shown in Fig. 8). A decrease in attenuation enhances the generation of harmonics but a decrease in nonlinearity reduces the amount of wave distortion due to nonlinear propagation (and therefore the creation of harmonics). A decrease in the focusing gain reduces the pressure at the focus and causes reduction in harmonic generation. For the 1 and 3.3 MHz pulses the Gol'dberg number is about 81 and 24, respectively, at 26 °C. This indicates that the effects of nonlinearity significantly dominate over absorption. Therefore, at low frequencies the decrease in the harmonics with temperature is due to the combined effects of reduction in both the focusing gain and nonlinearity with temperature.

As the frequency increases, the effects of absorption become more pronounced and the Gol'dberg number decreases. The value of the Gol'dberg number is equal to 1.2 and 0.7 at 26 °C for pulses with transmit frequencies of 13 and 20 MHz, respectively. Although at high frequencies both the focusing gain and the nonlinearity decrease with temperature, the reduction of attenuation compensates their effects. Therefore, at high frequencies the harmonics increase with temperature due to the significant decrease in absorption as a function of temperature. The change of

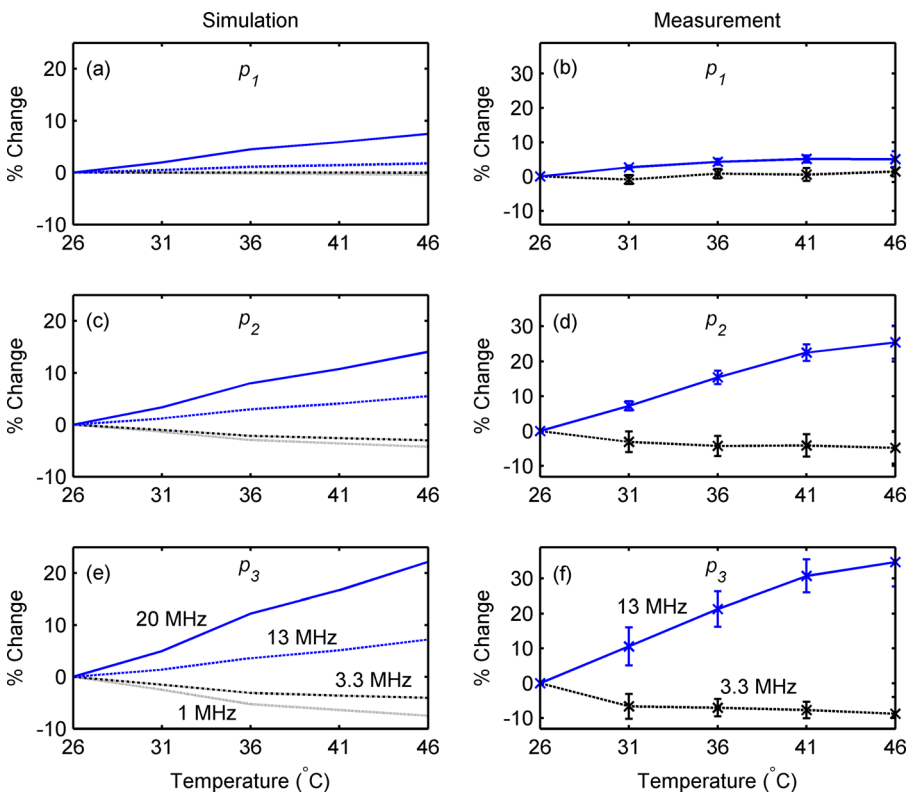

FIG. 6. (Color online) Simulated (left column) and measured (right column) changes in (a) and (b) p_1, (c) and (d) p_2, (e) and (f) p_3 as a function of temperature with respect to the initial temperature (26 °C) for pulses with transmit frequencies of 1, 3.3, 13, and 20 MHz. Measurements (right column) were only performed at two frequencies of 3.3 and 13 MHz. The error bars represent the standard deviation of 12 independent trials.

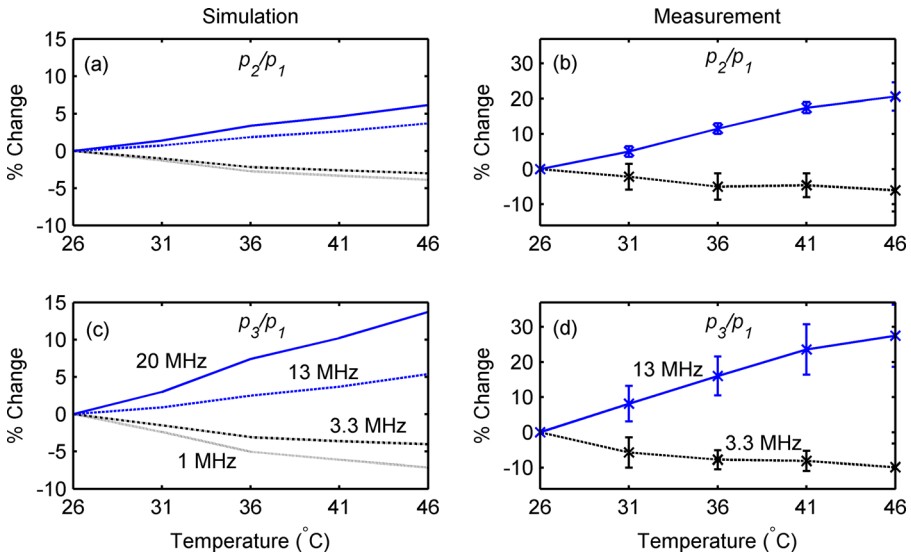

FIG. 7. (Color online) Simulated (left column) and measured (right column) changes in (a) and (b) p_2/p_1, (c) and (d) p_3/p_1 as a function of temperature with respect to the initial temperature (26 °C) for pulses with transmit frequencies of 1, 3.3, 13, and 20 MHz. Measurements (right column) were only performed at two frequencies of 3.3 and 13 MHz. The error bars represent the standard deviation of 12 independent trials.

harmonics with temperature better follow the temperature dependence of the Gol'dberg number.

Figures 6 and 7 show that higher harmonics have a higher sensitivity to temperature change. For the 1 and 3.3 MHz transmit frequencies, the higher the harmonic number, the steeper the decrease of the harmonics amplitude and their ratios with temperature. On the other hand, at 13 and 20 MHz, the higher the harmonic number, the steeper is the slope of the increase in the harmonic amplitudes and their ratios as the temperature increases from 26 °C to 46 °C. Keck and Beyer,[3,20] have shown that for a finite-amplitude plane wave propagating in an attenuating medium, the nth harmonic pressure amplitude is proportional to $[\beta/(\alpha_0\rho_0{c_0}^3)]^{n-1}$. Therefore, the temperature dependence of the acoustic parameters manifests themselves more prominently in the higher harmonics. Figure 9 shows the percentage change of $[\beta/(\alpha_0\rho_0{c_0}^3)]^{n-1}$ as a function of temperature for the harmonics at 13 MHz. This demonstrates that the higher harmonics are more sensitive to temperature.

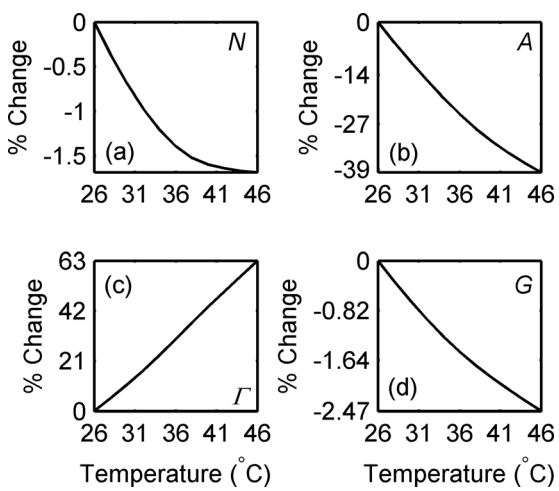

FIG. 8. The percentage changes in (a) the nonlinear parameter (N), (b) the absorption parameter (A), (c) the Gol'dberg number (Γ), and (d) the focusing gain (G) as a function of temperature for pulses with transmit frequencies of 1, 3.3, 13, and 20 MHz.

The increasing trend of the harmonics and their ratios with temperature at 13 MHz are consistent with those obtained in tissue-mimicking gel phantoms and *ex vivo* bovine muscle at the same transmit frequency (Maraghechi *et al.*[11]).

Figures 6 and 7 demonstrate that the trend of harmonics amplitudes and their ratios with temperature is similar in both the measurements and simulations. The results obtained from simulations at 3.3 MHz are within the standard deviation of the results obtained from measurements. However, the difference in the magnitude of the changes between simulations and experiments is more significant at 13 MHz. This could be due to approximations in values of acoustic parameters of water as a function of temperature as input in the simulations. The differences between measurements and simulations could also be due to measurement errors, since the acoustic field was manually scanned. The variation of frequency response with temperature of a typical hydrophone, such as the one we used in our study, could also be a possible reason for the mismatch between measurements and simulations.

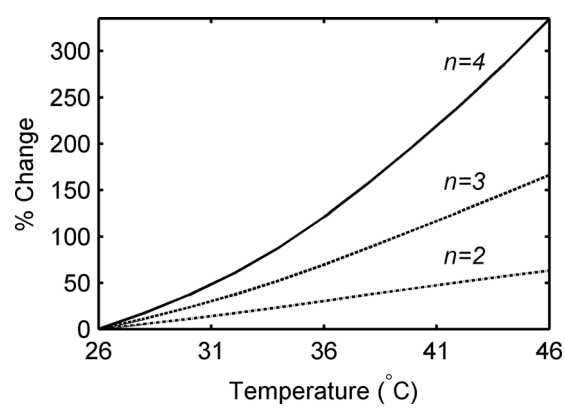

FIG. 9. The percentage change of $[\beta/(\alpha\rho_0{c_0}^3)]^{n-1}$ as a function of temperature for the second ($n=2$), third ($n=3$), and fourth ($n=4$) harmonics at 13 MHz transmit pulse frequency.

V. CONCLUSION

In this work, the temperature dependence of acoustic harmonics generated by nonlinear ultrasound wave propagation was investigated in water for a range of pulse transmit frequencies from 1 to 20 MHz. Measurements were conducted using two single element transducers to transmit the acoustic pressure signals and a calibrated hydrophone to receive them. The temperature-dependent KZK nonlinear ultrasound beam simulations were performed for the same experimental geometry. Several conclusions can be drawn from the results obtained in this study:

(1) The harmonics generated by nonlinear ultrasound wave propagation in water are temperature dependent.
(2) The temperature dependence of the harmonics generation is different for various transmit pulse frequencies. The temperature dependence of harmonics generated by nonlinear ultrasound wave propagation decreases with increasing temperature at 1 and 3.3 MHz while the opposite temperature dependence is observed at 13 and 20 MHz. The harmonics and the harmonic ratios at 1 and 20 MHz are more sensitive to temperature change compared to those at 3.3 and 13 MHz.
(3) The temperature dependence of harmonics depends on absorption, nonlinearity, and focusing gain.
(4) For a given transmit frequency, the higher the harmonic number, the higher is its sensitivity to temperature.
(5) The change in the harmonic generation as a function of temperature shows similar trends in both simulations and experiments at 3.3 and 13 MHz. However, there is a discrepancy between simulation and measurement results at 13 MHz.

It should be noted that the conclusions mentioned above depend strongly on the source parameters (transducer geometry, source pressure amplitude, and frequency) used in this study. In particular, characteristics of a nonlinear field depend on the source pressure amplitude. Varying the source pressure amplitude could therefore lead to some changes in the reported results. An extension of this work to investigate the effect of source pressure amplitude on harmonics generation with varying temperature will be the topic of the next project in this study.

ACKNOWLEDGMENTS

The authors wish to acknowledge technical assistance from Arthur Worthington from the Department of Physics, Ryerson University, Toronto, Canada. This work was partially supported by the Ontario Ministry of Research and Innovation Research Fund-Research Excellence (ORF-RE) grant, and the Natural Sciences and Engineering Research Council of Canada (NSERC Discovery grants) that were awarded to J.T. and M.C.K. Funding to purchase the equipment was provided by the Canada Foundation for Innovation, Canada Research Chairs program, and Ryerson University.

[1]R. M. Arthur, W. L. Straube, J. W. Trobaugh, and E. G. Moros, "Non-invasive estimation of hyperthermia temperatures with ultrasound," Int. J. Hyperthermia **21**, 589–600 (2005).
[2]M. A. Lewis, R. M. Staruch, and R. Chopra, "Thermometry and ablation monitoring with ultrasound," Int. J. Hyperthermia **31**, 163–181 (2015).
[3]M. F. Hamilton and D. T. Blackstock, *Nonlinear Acoustics* (Academic Press, San Diego, CA, 1998), pp. 54–139.
[4]F. A. Duck, "Nonlinear acoustics in diagnostic ultrasound," Ultrasound Med. Biol. **28**, 1–18 (2002).
[5]T. L. Szabo, *Diagnostic Ultrasound Imaging: Inside Out* (Academic Press, Oxford, 2014), Chap. 12, pp. 501–546.
[6]A. Bouakaz and N. de Jong, "Native tissue imaging at superharmonic frequencies," IEEE Trans. Ultrason. Ferroelectr. Freq. Control **50**, 496–506 (2003).
[7]D. Zhang, X. F. Gong, and X. Chen, "Experimental imaging of the acoustic nonlinearity parameter B/A for biological tissues via a parametric array," Ultrasound Med. Biol. **27**, 1359–1365 (2001).
[8]K. W. A. van Dongen and M. D. Verweij, "A feasibility study for non-invasive thermometry using non-linear ultrasound," Int. J. Hyperthermia **27**, 612–624 (2011).
[9]X. Liu, X. Gong, C. Yin, J. Li, and D. Zhang, "Noninvasive estimation of temperature elevations in biological tissues using acoustic nonlinearity parameter imaging," Ultrasound Med. Biol. **34**, 414–424 (2008).
[10]E. A. Both, "Feasibility study of temperature estimation based on nonlinear acoustics," M.Sc. dissertation, Delft University of Technology, 2010.
[11]B. Maraghechi, M. C. Kolios, and J. Tavakkoli, "Temperature dependence of nonlinear acoustic harmonics in *ex vivo* tissue and tissue-mimicking phantom," Int. J. Hyperthermia **31**, 666–673 (2015).
[12]Y. S. Lee and M. F. Hamilton, "Time-domain modeling of pulsed finite amplitude sound beams," J. Acoust. Soc. Am. **97**, 906–917 (1995).
[13]M. H. Hasani, S. Gharibzadeh, Y. Farjami, and J. Tavakkoli, "Unmitigated numerical solution to the diffraction term in the parabolic nonlinear ultrasound wave equation," J. Acoust. Soc. Am. **134**, 1775–1790 (2013).
[14]R. S. C. Cobbold, *Foundation of Biomedical Ultrasound* (Oxford University Press, New York, 2007), Chap. 1, pp. 12–74.
[15]M. J. Choi, S. R. Guntur, J. M. Lee, D. G. Paeng, K. I. L. Lee, and A. Coleman, "Changes in ultrasonic properties of liver tissue *in vitro* during heating-cooling cycle concomitant with thermal coagulation," Ultrasound Med. Biol. **37**, 2000–2012 (2011).
[16]E. J. Jackson, C.-C. Coussios, and R. O. Cleveland, "Nonlinear acoustic properties of ex vivo bovine liver and the effects of temperature and denaturation," Phys. Med. Biol. **59**, 3223–3238 (2014).
[17]R. T. Beyer, "Parameter of nonlinearity in fluids," J. Acoust. Soc. Am. **32**, 719–721 (1960).
[18]B. Zeqiri and A. D. Bond, "The influence of wave-form distortion on hydrophone spatial-averaging corrections—Theory and measurement," J. Acoust. Soc. Am. **92**, 1809–1821 (1992).
[19]M. S. Canney, M. R. Bailey, L. A. Crum, V. A. Khokhlova, and O. A. Sapozhnikov, "Acoustic characterization of high intensity focused ultrasound fields: A combined measurement and modeling approach," J. Acoust. Soc. Am. **124**, 2406–2420 (2008).
[20]W. Keck and R. T. Beyer, "Frequency spectrum of finite amplitude ultrasonic waves in liquids," Phys. Fluids **3**, 346–352 (1960).